CrossMark

Reduction mechanism of WO_3 + CuO mixture by combined Mg/C reducer

Non-isothermal conditions—high heating rates

S. V. Aydinyan[1,2,3] · Kh. T. Nazaretyan[1] · A. G. Zargaryan[1] · M. E. Tumanyan[1] · S. L. Kharatyan[1,2]

Abstract

The mechanism and kinetics of tungsten and copper oxides joint reduction by Mg + C combined reducer was studied at high heating rates by thermal analysis method utilizing high-speed temperature scanner. The effective values of activation energy for magnesiothermic reduction stage for the binary (WO_3–Mg, CuO–Mg), ternary (WO_3–Mg–C, CuO–Mg–C, WO_3–CuO–Mg) and quaternary (WO_3–CuO–Mg–C) systems were determined in a new and wide range of heating rates (V_h = 100–5200 °C min^{-1}). It was shown that for all the systems under study the increasing of heating rate shifts T^* values toward to high-temperature area and unlike the low heating rates (V_h = 5–20 °C min^{-1}, DTA/DTG studies) at high heating rates Mg always participates in molten state. In addition, by varying heating rates of reagents it was possible to separate the main stages and analyze intermediate compounds, making useful tool for the exploration of interaction mechanism in the complex systems. On the other hand, the tendency of merging of metals reduction stages at higher heating rates has an essential practical interest. That is, simultaneous reduction in metals is very prominent for obtaining metal composites with more homogeneous microstructure.

Keywords Metal oxides reduction · Mg/C combined reducer · High-speed temperature scanner · High heating rate · Activation energy

Introduction

During the last two decades, an increased interest has been paid to pseudoalloys based on Cu–refractory metal system (such as Cu–W, Cu–Mo, Cu–Cr) [1–5]. Their unique properties and multiple functionalities make them ideal for numerous high-tech applications, e.g., for instrumentation and portable equipment industries [6–10]. The development of new preparation methods of Cu–W composite materials for thermal management with high physicomechanical properties and bulk density is in the focus of modern research, as their characteristics highly depend on microstructure and phase composition of alloys. A number of novel technologies have been developed to enhance Cu–W composite densification ability by using finer precursors, such as homogeneously mixed tungsten and copper oxides/salts [11–19]. Generally, WO_3–CuO powder mixtures grinded in ball mill and reduced at 600–1000 °C up to 10 h in the hydrogen atmosphere, which is energy-consuming process and accompanied with undesirable growth of Cu grains, as well as result in drastic decrease in process efficiency. In our previous works [20–22], a separate and joint reduction of tungsten/molybdenum and copper oxides by energy-saving combustion synthesis was performed using Mg + C mixture as combined reducer. The using of such reducing mixture

✉ S. V. Aydinyan
  sofiya.aydinyan25@gmail.com

1 Laboratory of Kinetics of SHS Processes, A.B. Nalbandyan Institute of Chemical Physics NAS RA, 5/2, P. Sevak Str., 0014 Yerevan, Armenia

2 Department of Inorganic and Analytical Chemistry, Yerevan State University, 1, A. Manoogian Str., 0025 Yerevan, Armenia

3 Present Address: Material and Industrial Engineering, Tallinn University of Technology, Ehitajate tee 5, 19086 Tallinn, Estonia

allowed to control the reaction temperature in a wide range and to synthesize separate metals (W, Mo, Cu) or W(Mo)–Cu composite powders in a controllable combustion mode. However, considering that combustion processes are characterized by high temperatures and high self-heating rates of substances in the combustion front, considerable difficulties arise for exploring the interaction mechanism of the combustion process. Note that, according to the available literature data, the mechanism of joint reduction of WO_3 and CuO was not studied at all. To fill the gap, one of the approaches is the modeling of the process at controllable conditions (e.g., with programmed heating rates and tuning the process within the time) by using thermal analysis methods. This approach provides an enhanced opportunity to reveal the stepwise nature of complex reactions in the multicomponent systems.

In this paper are thoroughly outlined the results of investigation of the mechanism and kinetics of tungsten and copper oxides joint reduction by Mg + C mixture at programmed and high heating rates by thermal analysis method, utilizing the so-called high-speed temperature scanner (HSTS) developed by our research group [23–25]. At the last stage of the work, experiments performed at various heating rates (V_h = 100–5200 °C min^{-1}) allow to calculate the kinetic parameters (effective values of activation energy) for magnesiothermic reduction stage for the binary, ternary and quaternary systems.

Experimental

The following powders were used as raw materials: WO_3 (High grade, Pobedit Company, Russia, particle size less than 15 μm), CuO (High grade, STANCHEM, Poland, particle size less than 40 μm), magnesium powder (MPF-3, Russia, 150–300-μm particle size) and carbon black (P-803, Russia, particle size less than 1 μm).

Fig. 1 Overall view of the HSTS-2 experimental setup: *1*—Foil heater with reactive mixture and thermocouple. *2*—Reaction chamber. *3*—PC-assisted controller

HSTS setup (Fig. 1, Table 1) is designed for the kinetic investigations of the powdered mixtures under high heating rates (up to 10,000 °C min^{-1}) and temperature up to 1300 °C, which are more close to heating rates and temperatures in the combustion wave. The sequence of the experimental steps is as follows: Reactive powder mixture is placed into the metallic envelope made from thin metallic foil (e.g., Ni foil with 0.05–0.1 mm thickness), and a K-type thermocouple (chromel–alumel) is welded to the foil in central area of powder location. Note that for each experiment a new envelope is used, which is assumed to be inert at the given experimental conditions. The as-prepared envelope is fixed between massive electrodes into reaction chamber. Then, the latter is sealed, evacuated, purged with nitrogen and filled with 1 atm inert gas (Ar, 99.8%, purity < 0.1% O_2). The foil heater is preheated by passing electric current with desired temperature time schedule provided by PC-assisted controller. In this work, the linear preheating regime was used at heating rates ranging between 100 and 5200 °C min^{-1}. The so-called inert preheating of the envelope (after the reaction was accomplished) is also conducted for calibration purpose. Typical temperature profiles for the inert experiment provide linear temperature time profile, which defines the heating rate and coincides with the reactive T profile at low-temperature region when the reaction does not occur. The deviation temperature of the reactive profile from the inert one can be denoted as exo- or endothermic reactions proceeding in the reactive mixture. The reaction onset temperature (T_o), the maximum peak temperature observed during self-heating (T_{max}) and the temperature prescribed by linear heating, where the maximum exothermic effect is observed (T^*), are determined from the heating thermograms. Along with registration of temperature–time history, the setup allows to interrupt the process by turning off the electric current at different characteristic stages and the cooled samples subject to XRD analysis. At that cooling took place with high rate (up to 12,000 °C min^{-1}), which practically excluded further interaction during the cooling stage.

The intermediate (quenched) and final products were examined by XRD analysis method with monochromatic CuKα radiation (diffractometer DRON-3.0, Burevestnik, Russia) operated at 25 kV and 10 mA.

Results

The study of interaction mechanism in the CuO–WO$_3$–Mg–C system at high heating rates

To reveal the influence of heating rate and temperature on the interaction mechanism, the HSTS studies were performed at heating rates region from 100 up to

Table 1 Main characteristic parameters of HSTS-2 setup

Reagents	Powders
Heater	Ni foil, 40 × 12 mm, thickness 0.05–0.1 mm
Sample mass	5–100 mg
Sample heating rate	10–10,000 °C min^{-1}
Temperature range	20–1300 °C
Frequency of measurements and tracking	50 Hz
Sample cooling rate	up to 12,000 °C min^{-1}
Atmosphere	Vacuum, air, inert gas
Pressure	0–2 MPa

$V_h = 5200$ °C min^{-1} and $T_{max} = 1300$ °C. Firstly, binary (CuO–Mg, WO₃–Mg) and ternary (CuO–Mg–C, WO₃–Mg–C, CuO–WO₃–Mg) systems were studied at the same conditions considering only magnesiothermic or magnesiocarbothermic reduction reactions. The pure/solely carbothermic reduction processes are not discussed in this paper due to their low exothermicity and because of HSTS method is more sensitive to high exothermic reactions. Note that, in our previous works [26–30], some of these binary and ternary systems were studied at low heating rates using DTA/TG technique.

Based on the results obtained by HSTS investigations, the kinetic parameters (effective values of activation energy) are calculated for magnesiothermic reduction stage for all studied mixtures. There are several approaches for calculating the effective activation energy for non-isothermal experiments. One of the best known methods is isoconversion method formulated by Kissinger–Akahira–Sunose (KAS) [31]. In this method, the activation energy is calculated based on the shift of T_{max} on the temperature curve depending on the heating rate (V_h):

$$\ln\left(\frac{V_h}{\left(T_{max}^{DTA}\right)^2}\right) = \ln A - \frac{E}{R}\left(\frac{1}{T_{max}^{DTA}}\right)$$

where V_h is the heating rate (K min^{-1}), T_{max}^{DTA} is the magnesiothermic reduction temperature corresponding to the maximum advance of the DTA curve (K), A is a constant, E is the effective activation energy of the process and R is the universal gas constant. Note that the exothermic peak observed at $T > T_o$ is attaining a maximum value (T_{max}) corresponding to the temperature T^* on the inert profile. Thus, the difference $\Delta T = T_{max} - T^*$ defines the temperature change owing to the heat release of reaction, and for simple approximation T^* is used as the reaction temperature in KAS equation to determine kinetic parameters of the reaction. Regarding the multistage character of the process, effective activation energy values were calculated for joint or separate magnesiothermic reduction processes of WO₃ and CuO oxides.

Me–Mg and Me–C binary systems

CuO–Mg system

The exothermic interaction in the CuO–Mg binary system (CuO + 0.5Mg) starts immediately after the magnesium melting ($T_o = 665$ °C) and accompanied by the formation of Cu (Cu₂O) and MgO (Fig. 2) with peak temperature $T_{max} = 1285$ °C under $V_h = 300$ °C min^{-1} heating rate conditions. The amount of magnesium was limited in the initial mixture, as in the case of CuO + Mg reaction proceeds very violently and is difficult to perform measurement and registration.

As it was expected, the increase in heating rate from 100 to 1200 °C min^{-1} for the same reaction CuO + 0.5Mg increases T^* value (Table 2), allowing to calculate activation energy of solid–liquid interaction by using KAS equation. The value of $E_a = 424 \pm 25$ kJ mol^{-1} was obtained.
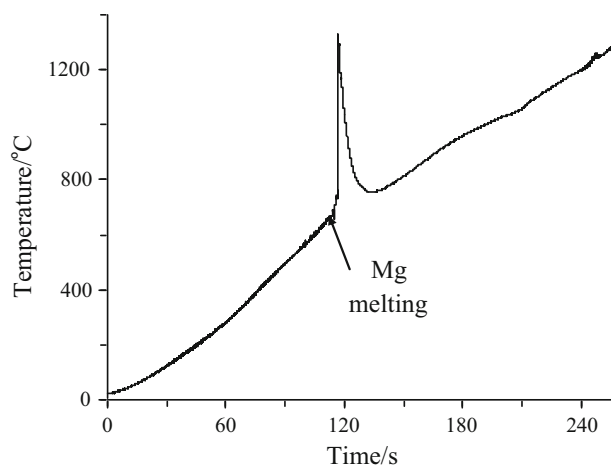
Fig. 2 Heating thermogram of the CuO + 0.5Mg mixture. $m_o = 30$ mg. $V_h = 300$ °C min^{-1}

Table 2 The characteristic peak shift T^* temperatures of the CuO + 0.5Mg, CuO + 0.5Mg + 0.25C, WO_3 + 3Mg, WO_3 + 1.5Mg + C reactions at various heating rates, V_h, and effective activation energy values calculated on their bases

V_h/°C min^{-1}	CuO + 0.5Mg $E_a = 424 \pm 25$ kJ mol^{-1} T^*/°C	WO_3 + 3Mg $E_a = 106 \pm 6$ kJ mol^{-1} T^*/°C	CuO + 0.5Mg + 0.25C $E_a = 320 \pm 19$ kJ mol^{-1} T^*/°C	WO_3 + 1.5Mg + C $E_a = 92 \pm 5$ kJ mol^{-1} T^*/°C
2600	–	–	803	931
1200	748	803	786	838
600	733	714	770	760
300	718	675	745	720
150	711	661	730	675
100	700	637	720	658

WO$_3$–Mg system

Magnesiothermic reduction of tungsten (VI) oxide in the mixture (WO_3 + 3Mg) is a highly exothermic process, which is characterized by one sharp exothermic peak and similar to the CuO–Mg interaction also initiates immediately after the magnesium melting at 660 °C. At 300 °C min^{-1} heating rate, the peak temperature was 1250 °C (maximum self-heating makes about 600 °C).

Note that at low heating rates (2.5–20 °C min^{-1}, DTA/TG experiments) the magnesiothermic reduction of WO_3 starts at $T \approx 560–630$ °C [26]. In this case, the most important factor is the fact that intensive interaction takes place below the melting point of Mg and undergoes by solid + solid scheme. Thus, increasing the heating rate leads to the considerable shift of T_o and T^* toward higher temperature range. Regardless the heating rate, WO_3 reduction proceeds completely with formation of metallic tungsten and MgO. E_a value calculated for WO_3 + Mg reaction from the results (Table 2) for high heating rates (106 ± 6 kJ mol^{-1}, solid + liquid interaction) is significantly lower, than that obtained by DTA method (153.1 kJ mol^{-1}, solid + solid interaction). Thus, the transition of the reaction WO_3 + 3Mg from low-temperature area with solid + solid mechanism to the high-temperature one with solid + liquid mechanism results in lowering of the activation energy by the factor 1.5.

WO$_3$–Mg–C, CuO–Mg–C and WO$_3$–CuO–Mg ternary systems

CuO–Mg–C system

The reduction process in the CuO–Mg–C system at $V_h = 300$ °C min^{-1}, analogous to the aforementioned systems, starts immediately after magnesium melting. First of all, copper oxide carbothermic reduction occurs producing copper suboxide (650–750 °C), followed by magnesiothermic reduction at 750–780 °C (Fig. 3a). At the end

of the reaction, completely reduced copper is present (Fig. 3b). Such sequence of reduction is asserted by the presence of Mg and the absence of MgO in XRD pattern of the quenched product at point A (Fig. 3b).

Table 2 shows corresponding T^* values for magnesiothermic stage of the CuO + 0.5Mg + 0.25C mixture at various heating rates. Based on data present in Table 2, the effective activation energy for the magnesiothermic stage was estimated ($E_a = 320 \pm 19$ kJ mol^{-1}). Based on the results of XRD analysis, it represents the effective activation energy for the reaction Cu_2O + 0.5Mg.

WO$_3$–Mg–C system

The chemical interaction in the WO$_3$–Mg–C system also begins immediately after the magnesium melting and then continues along the rise in temperature (Fig. 4a). It should be noted that tungsten is completely reduced at the end of the reaction (Fig. 4b, D). Note that at WO_3 reduction by (Mg + C) binary mixture at lower heating rates (DTA/TG, V_h = 5–20 °C min^{-1}) a very weak carbothermal reduction takes place at least up to 800 °C, and in contrast to high heating rates the interaction between Mg and WO_3 takes place in the solid state at $T < T_{Mg\ melt}$.

For the WO_3 + 1.5Mg + C mixture, the effective activation energy for the magnesiothermic reduction stage makes about 92 ± 5 kJ mol^{-1}, which is only a little less than that for solely magnesiothermic reduction (see Table 2).

On the other hand, compared with the E_a value of WO_3 + 1.5Mg + C reaction calculated for the low heating rates (DTA/TG, $E_a = 177.4$ kJ mol^{-1}), it is lower about two times, supporting the statement that at low and high heating rates interaction in these systems occurs by different mechanisms. Thus, at low heating rates (DTA/TG, V_h = 5–20 °C min^{-1}) interaction proceeds by the solid + solid mechanism with $E_a = 177.4$ kJ mol^{-1}, and by the mechanism of solid + liquid at high heating rates ($V_h > 100$ °C min^{-1}) with $E_a = 92 \pm 5$ kJ mol^{-1}.

Fig. 3 Heating thermogram of the CuO + 0.5Mg + 0.25C mixture at $V_h = 300$ °C min^{-1}, $m_o = 50$ mg (**a**) and XRD pattern of products quenched at characteristic temperatures. A— $T = 750$. B—1300 °C (**b**)
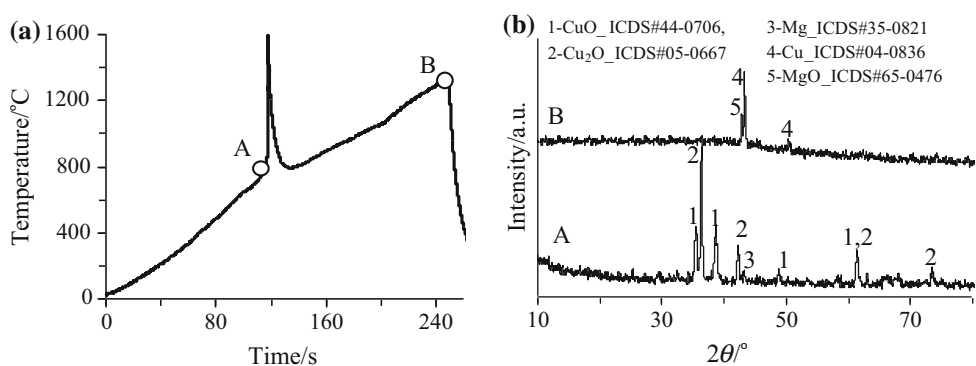
Fig. 4 Heating thermogram of the WO₃ + 1.5Mg + C mixture at $V_h = 300$ °C min^{-1}, $m_o = 50$ mg (**a**) and XRD pattern of products quenched at characteristic temperatures: A— $T = 655$. B—900. C—1070. D—1300 °C (**b**)
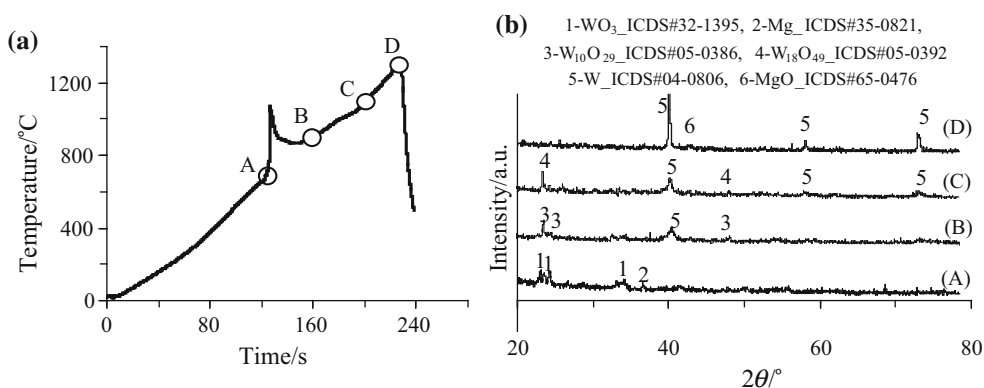
WO₃–CuO–Mg system

According to the results obtained for the CuO + WO₃ + 4Mg mixture, no interaction occurs before magnesium melting (Fig. 5a, b). The results of XRD analysis for the sample cooled at 610 °C (A) indicate only the presence of the initial reagents, CuO, WO₃ and Mg (Fig. 5b). Just after magnesium melting, copper oxide is reduced into the suboxide and then up to metallic copper (points B, C). At temperatures higher than 850 °C, reduction of tungsten (VI) oxide starts. However, according to XRD analysis results, for the sample cooled at 1035 °C

tungsten oxide is reduced partially (point D), the complete reduction takes place at 1300 °C (point E).

Note that, according to [29], the magnesiothermic reduction in the both oxides at low heating rates (DTA/TG, $V_h = 5$–20 °C min^{-1}) occurs jointly at the same temperature interval: The reaction begins before magnesium melting at 620 °C, and the maximum value for the temperature shifting corresponds to $T_{max} = 647$ °C, while at heating rate $V_h > 100$ °C min^{-1} these two stages are clearly separated and proceeded after the Mg melting.

The significant influence of heating rate on the thermograms (e.g., T shift of characteristic stages, merging of stages and change in intensity) was observed; numeric

Fig. 5 Heating thermogram of the CuO + WO₃ + 4Mg mixture ($V_h = 300$ °C min^{-1}, $m_o = 45$ mg) (**a**) and XRD patterns of the CuO + WO₃ + 4Mg mixture after process interruption at different temperatures: A— T = 610. B—670. C—850. D— 1035. E—1310 °C (**b**)
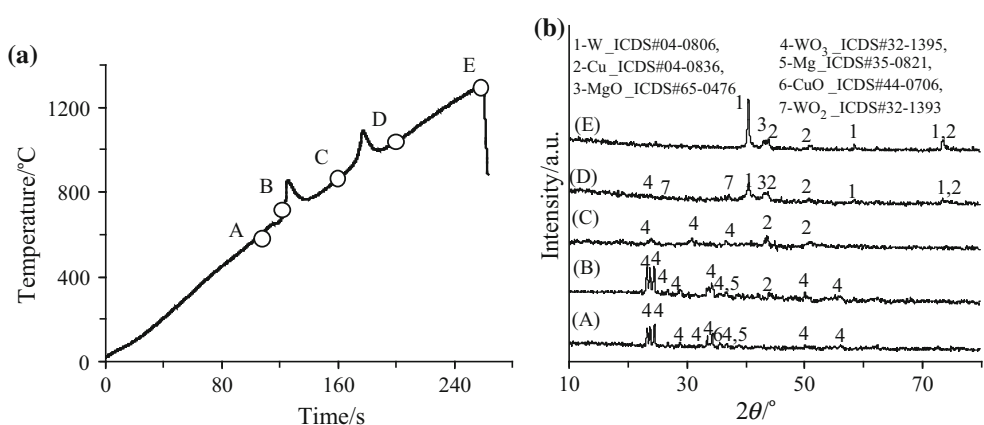
values are illustrated in Table 3. It was shown that increasing the heating rate contributes to the approaching of individual stages, and at $V_h > 390\ °C\ min^{-1}$ their fully merging occurs similar to that at low heating rates (2.5–20 °C min^{-1}). In this instance, at rather high heating rates the re-merging of stages is associated with a substantial increase in the self-heating observed during the first stage. Furthermore, the second stage starts at that high temperature before the completion of the first stage; thus, T_{max} of the first stage exceeds to T_o of the second stage.

At further increasing of heating rate, T^* shifts to the higher temperature area allowing to calculate effective activation energy of overall magnesiothermic process ($E_a = 260 \pm 16\ kJ\ mol^{-1}$). Besides, at heating rates $100 < V_h < 390\ °C\ min^{-1}$ the values of activation energy for individual stages was also possible to calculate due to clearly separated stages of reduction in individual oxides. The E_a value for magnesiothermic reduction in copper oxide makes about $248 \pm 15\ kJ\ mol^{-1}$ (1st stage) in the presence of tungsten oxide, while pure CuO + Mg reduction was characterized by higher E_a value. Tungsten oxide reduction by Mg occurs at the second stage in the presence of copper with $E_a = 64 \pm 4\ kJ\ mol^{-1}$.

WO$_3$–CuO–Mg–C quaternary system

Experiments performed with the quaternary CuO + WO$_3$ + 2.5Mg + 1.5C system showed that the multistage reduction process starts also after magnesium melting (Fig. 6a). At that, firstly a weak exothermic interaction takes place corresponding to the reduction of copper by carbon, which was confirmed by XRD analysis data for the sample cooled at 770 °C (Fig. 6b, B). A weakly exothermic carbothermal reduction is followed by a sharp exothermic magnesiothermic one, which goes to end at 830 °C, and appropriate diffraction pattern indicates to Cu, W, WO$_3$, WO$_2$ and MgO (Fig. 6b, C). Note that at higher temperatures (point D) complete reduction of tungsten was observed. The latter is possible if the carbon also participates in the reduction process in the C–D area. Thus, reduction in the oxides mixture under consideration begins

with carbothermic reduction of copper oxide, followed by magnesiocarbothermic reduction of tungsten oxide.

With the increasing of heating rate, T^* values shift to the higher temperature area allowing to calculate effective activation energy of magnesiocarbothermic reduction process (Fig. 7). The value of $E_a = 150 \pm 9\ kJ\ mol^{-1}$ was obtained, which is quite less than that for metal oxides joint reduction by Mg and significantly higher than Mg reduction of WO$_3$.
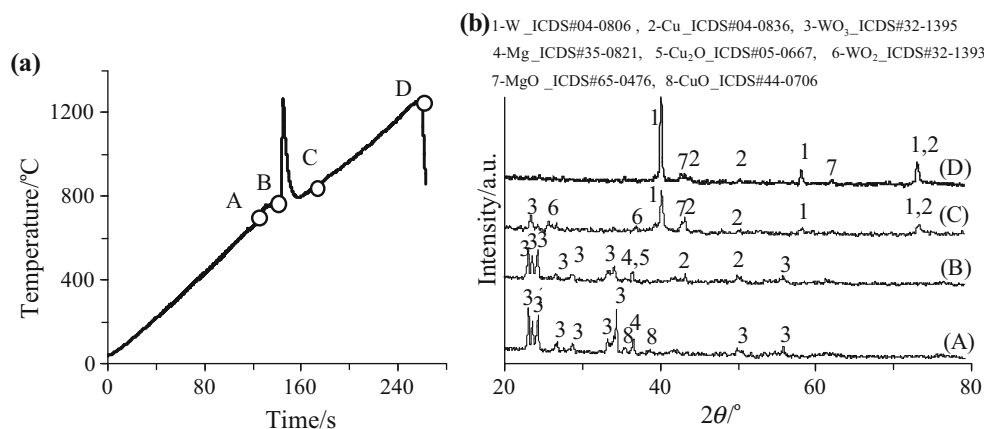
Discussion

Thus, the mechanism of reduction in the CuO–WO$_3$–Mg–C system in a wide range of high heating rates (100–5200 °C min^{-1}) was examined by HSTS technique, comparative overview with low heating rate (DTA method) was done, and the dramatic influence of the heating rate on the appearance of various stages, maximum peak temperature, temperature shift, etc., was revealed. For the first time, an effective kinetic data have been gathered through the applied approach in a completely new range of heating rates (100–5200 °C min^{-1}) for the surveyed systems, which is of great interest to the mechanism and kinetics of non-isothermal processes. Note that the obtained activation energies are generally presented as effective values for overall process or individual steps allowing to characterize non-isothermal interactions under high heating rate conditions.

From the analysis and evaluation of the data obtained for binary, ternary and quaternary mixtures, it is apparent that magnesiothermic reduction peculiarities endured significant change and exhibit dramatically different nature for binary, ternary and quaternary systems.

Activation energy value obtained for the CuO + Mg solid–liquid interaction was calculated as $424 \pm 25\ kJ\ mol^{-1}$, which is characteristic for the thermite reactions. According to the literature, high effective activation energy values obtained for thermite reactions are rationalized in terms of the high-temperature requirement for ignition of the thermite reaction and its high reaction rates. In the comparative overview about the thermite reactions [32],

Table 3 The characteristic peak shift T^* temperatures of the stepwise (I, II) and joint magnesiothermic reduction of WO$_3$ and CuO oxides at various heating rates, V_h, and effective activation energy values calculated on their bases

WO$_3$ + CuO + 4Mg I stage $E_a = 248 \pm 15\ kJ\ mol^{-1}$		WO$_3$ + CuO + 4Mg II stage $E_a = 64 \pm 4\ kJ\ mol^{-1}$		WO$_3$ + CuO + 4Mg Joint $E_a = 260 \pm 16\ kJ\ mol^{-1}$	
V_h/°C min^{-1}	T^*/°C	V_h/°C min^{-1}	T^*/°C	V_h/°C min^{-1}	T^*/°C
300	703	300	953	5200	907
200	692	200	892	2600	888
150	682	150	868	1200	862
130	678	130	835	600	830
100	672	100	809	390	810

Fig. 6 Heating thermogram of the CuO + WO$_3$ + 2.5Mg + 1.5C mixture (V_h = 300 °C min^{-1}, m_o = 50 mg) (**a**) and XRD patterns of the CuO + WO$_3$ + 2.5Mg + 1.5C mixture after process interruption at different temperatures: A—T = 660. B—770. C—830. D—1230 °C (**b**)
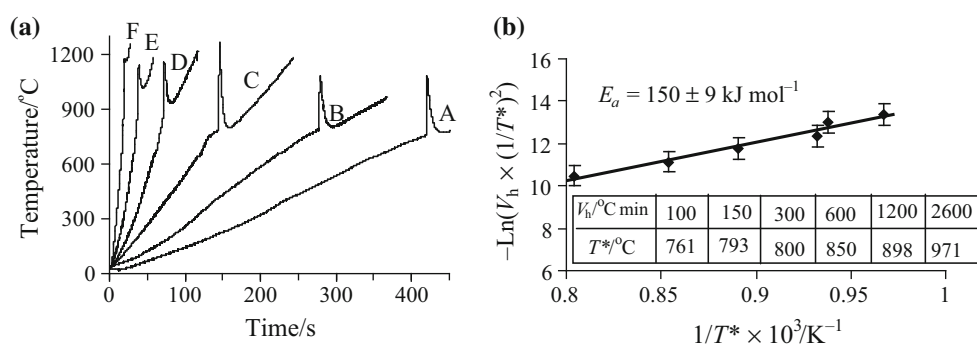
Fig. 7 Heating thermograms of the CuO + WO$_3$ + 2.5Mg + 1.5C mixture at various heating rates (**a**) and determination of activation energy (**b**). A—V_h = 100. B—150. C—300. D—600. E—1200. F—2600 °C min^{-1}

authors reported the activation energy of 658 kJ mol^{-1} of the aluminothermic reduction 3Cu$_2$O(s) + 2Al(s) = Al$_2$O$_3$(s) + 6Cu(s). In the CuO–Mg system, $E_a \sim 300$ kJ mol^{-1} was obtained depending on the conversion degree, besides it has a tendency of increase with the increasing of conversion degree [33]. Kinetic model of aluminothermic reduction of molybdenum (VI) oxide was investigated and extrapolated to high heating rates in the 10^3–10^6 K s^{-1} range [34]. The reaction was treated as a combination of four subreactions, which were described by a combination of a diffusion-controlled reaction model and first-order reactions. The activation energies determined in this study for each individual step are in the range of 209–373 kJ mol^{-1} [34]. In [35] reported that the increase in magnesium amount in the initial mixture increases the value of activation energy, for example, Al + 10%Mg–Fe$_2$O$_3$ reaction is characterized by E_a = 247 kJ mol^{-1}, while E_a = 312 kJ mol^{-1} for the Al + 30%Mg + Fe$_2$O$_3$ reaction. Based on the kinetic data, the Mg–CuO has higher activation energy than Al–Mg–CuO and Al–CuO systems [36]. Depending on the conversion degree, it varies between 270 and 300 kJ mol^{-1} for the CuO–Mg system.

It is worth mentioning that in the case of a magnesiothermic reduction in the oxides CuO + WO$_3$ mixture various behavior was observed at low (DTA, 5–20 °C min^{-1}) and high heating rates (HSTS, 100–400 °C min^{-1}). DTA studies showed that they proceed simultaneously in the same temperature interval ($T_o \sim 620–630$ °C) before the melting of Mg. HSTS experiments allowed to separate various stages in the CuO–WO$_3$–Mg system due to the high difference in their activation energies in a range of heating rates 100–400 °C min^{-1}; however, there is a tendency of merging of these stages again at higher heating rates.

In the ternary CuO–Mg–C, WO$_3$–Mg–C and quaternary CuO–WO$_3$–Mg–C mixtures at low and high heating rates as well, the reduction starts with carbon, then magnesium participates to the reduction. The addition of carbon in the binary or ternary system leads to T^* changes toward higher temperature range, which is in agreement with the results reported in [26, 28]. It was also confirmed that during the combined reduction of oxides by Mg/C reducing mixture often carbothermic reduction of oxides precedes magnesiothermic reaction or occurs earlier and faster leading to the incomplete reduction of oxides (e.g., CuO → Cu$_2$O or

$WO_3 \rightarrow WO_{3-x}$). Furthermore, magnesiothermic reduction in these partially reduced intermediates differs from solely magnesiothermic reaction of the initial oxides. In addition, at high heating rate region Mg took part always in molten state. Such behavior of carbon, as well as magnesium participation in liquid state in a new high heating rate region, provides a new pathway for the interaction in the WO_3–CuO–Mg–C system with lower effective activation energy than that for the WO_3–CuO–Mg system.

For all the systems under study, the increasing of heating rate shift T^* values toward the high-temperature area allowing to calculate effective activation energies of magnesio- and/or magnesiocarbothermic reduction processes.

In addition, by varying heating rates of reagents it is possible to separate the main stages and analyze intermediate compounds, making useful tool for the exploration of interaction mechanism in the complex systems. It is important to note that the tendency of merging of metals reduction stages at higher heating rates has also an essential practical interest. That is, simultaneous reduction in metals is very prominent for obtaining metal composites with more homogeneous microstructure.

Conclusions

The reduction mechanism in the binary (WO_3–Mg, CuO–Mg), ternary (WO_3–Mg–C, CuO–Mg–C, WO_3–CuO–Mg) and quaternary (WO_3–CuO–Mg–C) systems at non-isothermal conditions in a wide range of high heating rates (100–5200 °C min^{-1}) was examined by HSTS technique, and the results were compared with the mechanism at low heating rates (2.5–20 °C min^{-1}, DTA/DTG method). In all systems under the conditions of low heating rates (DTA, 5–20 °C min^{-1}), carbothermic and magnesiothermic reduction processes start before magnesium melting, in respect to that, at high heating rate region (HSTS, 100–5200 °C min^{-1}) Mg took part in interaction always in molten state. In addition, at higher heating rates the reduction stages of metals tend to re-merge and simultaneous reduction in metals takes place, promoting more homogeneous microstructure formation in composites. Using HSTS setup, effective kinetic data have been gathered in a completely new range of heating rates (100–5200 °C min^{-1}) for the first time, for the magnesiothermic and magnesiocarbothermic reduction processes of the CuO–Mg, CuO–Mg–C, WO_3–Mg, WO_3–Mg–C, CuO–WO_3–Mg and CuO–WO_3–Mg–C systems, which is of great interest to the mechanism and kinetics of non-isothermal processes. The effective activation energy value of the quaternary CuO–WO_3–Mg–C mixture was calculated to be 150 kJ mol^{-1}, which is lower in comparison with the joint magnesiothermic reduction reactions of CuO and WO_3, manifesting the decisive role of carbon addition on the interaction mechanism at high heating rates.

References

1. Habashi F. Alloys: preparation, properties, applications. New York: Wiley; 2008.
2. Selvakumar N, Vettivel SC. Thermal, electrical and wear behavior of sintered Cu–W nanocomposite. Mater Des. 2013;46:16–25.
3. Minakova RV, Lesnik ND, Kresanova AP, Flis AA, Khomenko EV. Contact interaction, structure, and properties of W (Mo, Cr)–Cu composites with additives. Powder Metall Met Cer. 1996;35(7):363–71.
4. Bukhanovs'kyi VV, Rudnyts'kyi MP, Kharchenko VV, Minakova RV, Grechanyuk MI, Mamuzic I. Relationship between composition, structure, and mechanical properties of a condensed composite of copper–tungsten system. Strength Mater. 2011;43(4):426–37.
5. Bukhanovskii VV, Minakova RV, Grechanyuk IN, Mamuziæ I, Rudnitskii NP. Effect of composition and heat treatment on the structure and properties of condensed composites of the Cu–W system. Met Sci Heat Treat. 2011;53(1-2):14–23.
6. Kaczmar JW, Pietrzak K, Włosiński W. The production and application of metal matrix composite materials. J Mater Process Technol. 2000;106(1):58–67.
7. Dorfman LP, Scheithauer MJ, Paliwal M, Houck DL, Spencer JR. Alloy for electrical contacts and electrodes and method of making. U.S. Patent No. 6,375,708; 2002.
8. Rani AM, Mahamat AZ, Ab Adzis AH. Novel nano copper-tungsten-based EDM electrode. In: Viswanatha Sharma K, Hisham B Hamid N, editors. Engineering applications of nanotechnology. Berlin: Springer; 2017. p. 193–224.
9. He L, Yu J, Duan W, Liu Z, Yin S, Luo H. Copper–tungsten electrode wear process and carbon layer characterization in electrical discharge machining. Int J Adv Manuf Technol. 2016;85(5-8):1759–68.
10. Guo TB, Zhao JY, Ding YT. Microstructure and properties of tungsten copper composite material. In: Materials science forum, vol 788. Trans Tech Publications; 2014, pp 646–51.
11. Chen CF, Pokharel R, Brand MJ, Tegtmeier EL, Clausen B, Dombrowski DE, Ickes TL, Lebensohn RA. Processing and consolidation of copper/tungsten. J Mater Sci. 2017;52(2):1172–82.
12. Daoush WM, Yao J, Shamma M, Morsi K. Ultra-rapid processing of high-hardness tungsten–copper nanocomposites. Scr Mater. 2016;113:246–9.
13. Xu L, Srinivasakannan C, Zhang L, Yan M, Peng J, Xia H, Guo S. Fabrication of tungsten–copper alloys by microwave hot pressing sintering. J Alloys Compd. 2016;658:23–8.
14. Lin D, Han JS, Kwon YS, Ha S, Bollina R, Park SJ. High-temperature compression behavior of W–10 wt% Cu composite. Int J Refract Met Hard Mater. 2015;53:87–91.
15. Duan L, Lin W, Wang J, Yang G. Thermal properties of W–Cu composites manufactured by copper infiltration into tungsten fiber matrix. Int J Refract Met Hard Mater. 2014;46:96–100.
16. Xi X, Xu X, Nie Z, He S, Wang W, Yi J, Tieyong Z. Preparation of W–Cu nano-composite powder using a freeze-drying technique. Int J Refract Met Hard Mater. 2010;28(2):301–4.
17. Basu AK, Sale FR. Copper-tungsten composite powders by the hydrogen reduction of copper tungstate. J Mater Sci. 1978;13(12):2703–11.

18. Raghu T, Sundaresan R, Ramakrishnan P, Mohan TR. Synthesis of nanocrystalline copper–tungsten alloys by mechanical alloying. Mater Sci Eng A. 2001;304:438–41.

19. Jech DE, Juan LS, Anthony BT. Process for making improved copper/tungsten composites. U.S. Patent No. 5,686,676; 1997.

20. Kirakosyan HV, Aydinyan SV, Kharatyan SL. W–Cu composite powders obtained by joint reduction of oxides in combustion mode. Int J SHS. 2016;25(4):215–23.

21. Aydinyan SV, Kirakosyan HV, Zakaryan MK, Kharatyan SL. Combustion synthesis of W–Cu composite powders from oxide precursors with various proportions of metals. Int J Refract Met Hard Mater. 2017;64:176–83.

22. Aydinyan SV, Kirakosyan HV, Kharatyan SL. Cu–Mo composite powders obtained by combustion-coreduction process. Int J Refract Met Hard Mater. 2016;54:455–63.

23. Nepapushev AA, Kirakosyan KG, Moskovskikh DO, Kharatyan SL, Rogachev AS, Mukasyan AS. Influence of high-energy ball milling on reaction kinetics in the Ni–Al system: an electrothermorgaphic study. Int J SHS. 2015;24(1):21–8.

24. Hobosyan MA, Kirakosyan KG, Kharatyan SL, Martirosyan KS. PTFE–Al₂O₃ reactive interaction at high heating rates. J Therm Anal Calorim. 2015;119(1):245–51.

25. Hobosyan MA, Kirakosyan KG, Kharatyan SL, Martirosyan KS. Study of dynamic features of highly energetic reactions by DSC and high-speed temperature scanner (HSTS). In: MRS proceedings. Cambridge University Press. 2013; p 1521.

26. Baghdasaryan AM, Niazyan OM, Khachatryan HL, Kharatyan SL. DTA/TG study of tungsten oxide and ammonium tungstate reduction by (Mg + C) combined reducers at non-isothermal conditions. Int J Refract Met Hard Mater. 2014;43:216–21.

27. Baghdasaryan AM, Niazyan OM, Khachatryan HL, Kharatyan SL. DTA/TG study of molybdenum oxide reduction by Mg/Zn & Mg/C combined reducers at non-isothermal conditions. Int J Refract Met Hard Mater. 2015;51:315–23.

28. Kirakosyan HV, Minasyan TT, Niazyan OM, Aydinyan SV, Kharatyan SL. DTA/TGA study of CuO and MoO₃ co-reduction by combined Mg/C reducers. J Therm Anal Calorim. 2016;123:35–41.

29. Niazyan OM, Aydinyan SV, Kharatyan SL. DTA/TG study of reduction mechanism of WO₃ + CuO mixture by combined Mg/C reducer. Chem J Armenia. 2016;69(4):399–406.

30. Aydinyan S, Kirakosyan H, Niazyan O, Tumanyan M, Nazaretyan Kh, Kharatyan S. Reaction pathway in the WO₃–CuO–Mg–C system at nonisothermal conditions. Armen J Phys. 2016;9(1):83–8.

31. Starink MJ. The determination of activation energy from linear heating rate experiments: a comparison of the accuracy of isoconversion methods. Thermochim Acta. 2003;404(1-2):163–76.

32. Wang LL, Munir ZA, Maximov YM. Review, Thermite reactions: their utilization synthesis and processing of materials. J Mater Sci. 1993;28:3693–708 **(Primary source: G.D. MILLER, Thermochim. Acta 34 (1979) 357)**.

33. Hosseini SG, Sheikhpour A, Keshavarz MH, Tavangar S. The effect of metal oxide particle size on the thermal behavior and ignition kinetic of Mg–CuO thermite mixture. Thermochim Acta. 2016. https://doi.org/10.1016/j.tca.2016.01.005.

34. Schoenitz M, Umbrajkar S, Dreizin EL. Kinetic analysis of thermite reactions in Al–MoO₃ nanocomposites. J Propuls Power. 2007. https://doi.org/10.2514/1.24853.

35. Wang Y, et al. Energy release characteristics of impact-initiated energetic aluminum–magnesium mechanical alloy particles with nanometer-scale structure. Thermochim Acta. 2011;512(1):233–9.

36. Sheikhpour A, Hosseini SG, Tavangar S, Keshavarz MH. The influence of magnesium powder on the thermal behavior of Al–CuO thermite mixture. J Therm Anal Calorim. 2017;129(3):1847–54. https://doi.org/10.1007/s10973-017-6343-z.